

Zero modes of the domain wall operator for 2+1 flavor lattices with $a^{-1} \approx 1$ GeV

Duo Guo^{*†}

Department of Physics, Columbia University, New York, NY 10027, USA

E-mail: dg2806@columbia.edu

The measurement of the topological properties on the lattices usually requires smearing. In this proceeding, we demonstrate that we can use the zero modes of the domain wall operator to study the topological properties in detail without smearing. We show that the eigenvalues and the chirality properties of the eigenvectors are very similar to those of the Dirac operator with mass term in the continuum. The finite fifth dimension brings the residual mass into the eigenvectors but the eigenvectors can still be used to probe the detailed topological properties. We are able to get the quark bilinear $\sum_{\vec{x}, \vec{y}} \langle \bar{q}(\vec{x}, t) \gamma_5 q(\vec{y}, t) \rangle$ through the eigenvectors which contribute to m_η and $m_{\eta'}$. m_η and $m_{\eta'}$ are measured and we expect that we can use the zero modes to improve the measurements.

37th International Symposium on Lattice Field Theory - Lattice2019

16-22 June 2019

Wuhan, China

^{*}Speaker.

[†]The author is grateful to Robert M. Mawhinney, David J. Murphy and Chulwoo Jung for helpful discussion in support of this work. Calculations were performed using the Blue Gene/Q computers of the RIKEN-BNL Research Center and Brookhaven National Lab. The software used includes the CPS QCD code, supported in part by the USDOE SciDAC program, the BAGEL assembler kernel generator for high-performance optimized kernels and fermion solvers. The author is supported in part by U.S. DOE grant #DE-SC0011941.

1. Introduction

The QCD vacuum has non-trivial topological properties which break the $U_A(1)$ symmetry [1]. The symmetry-breaking explains that the masses of η and η' are very different. Consequently, the measurements for η and η' require a good sampling over the topological sectors for the lattice QCD. However, the measurement of the topological properties on the lattices is difficult because the local fluctuation of the gauge fields is large. The common way to overcome the difficulty is to smear the field. However, the measurements for η and η' are done without smearing. Also, it only gives the global topological charge and doesn't give the details of the topological properties.

In [2], we found that for our 24ID $a^{-1} \approx 1 \text{ GeV}$ ensemble, even though the global topology is evolving fine, the autocorrelation time is long and the local topological properties are important. Here we develop the idea of using the zero modes of the domain wall operator to study the topological properties. In Section 2, we introduce the lattices and the calculation of the eigenvectors. In Section 3, we show the results of the eigenvectors. Particularly, we explain our understanding of the eigenvalues and the chirality of the domain wall eigenvectors. In Section 4, we demonstrate that we can use the low-lying eigenvectors to construct the quark bilinear that contributes to m_η and $m_{\eta'}$. We show the measurements for η and η' in section 5 and give the conclusion and the outlook in Section 6.

2. Lattices and calculation details

We consider three ensembles in this study. The action for the three ensembles is the the Iwasaki+DSDR (Dislocation Suppressing Determinant Ratio) gauge action [3]. The DSDR part suppresses the changes of the topological charges which is important when the coupling is strong. The three ensembles include the $24^3 \times 64$, $a^{-1} \approx 1 \text{ GeV}$ ensemble [3] with $m_\pi \approx 140 \text{ MeV}$, $24^3 \times 64$, $a^{-1} \approx 2 \text{ GeV}$ ensemble with $m_\pi \approx 300 \text{ MeV}$ and $12^3 \times 32$, $a^{-1} \approx 1 \text{ GeV}$ ensemble with $m_\pi \approx 300 \text{ MeV}$. For the eigenvectors, we use the implicitly restarted Lanczos algorithm to calculate eigenvectors for the 12ID ensemble and the Ritz algorithm to calculate the eigenvectors for the two 24ID ensembles. The information is listed in Table 1.

During the calculation of the eigenvectors, we use different inputs masses to study the mass dependence of the eigenvectors. We also varied the length of the fifth dimension, L_5 , for the 12ID ensemble. For the two 24ID ensembles, we only calculated on a few configurations due to the computation limits. More calculation is ongoing under our 2019 US-QCD project.

3. Properties of the low-lying eigenvectors

In this section we show the properties of the low-lying eigenvectors of the lattice Hermitian domain wall operator $\gamma_5 R_5 D$ where D is the Shamir Domain wall operator, R_5 is the reflection operator in the fifth dimension. We start from the continuum limit and consider the Dirac operator with the mass term. It'll be shown that the lattice operator with finite L_5 is very similar to the massive Dirac operator in the continuum because of the residual mass. Specifically, we consider the eigenvalues and chirality of the eigenvectors. The comparison between the topological charge calculated from the eigenvectors and the gauge fields is also done.

size	a^{-1}	m_π	total configurations	total eigenvectors	methods
12×32	1GeV	300MeV	70	3500	Lanczos
24×64	1GeV	140MeV	2	40	Ritz
24×64	2GeV	300MeV	2	60	Ritz

Table 1: Lattices and the eigenvectors

In the continuum, the massless Dirac operator $i\cancel{D}$ is Hermitian and it anticommutes with γ_5 . It follows that if the eigenvalue $\lambda = 0$, $\gamma_5 \psi_0 = \pm \psi_0$ and $\langle \psi_0 | \gamma_5 | \psi_0 \rangle = \pm 1$. If $\lambda \neq 0$, $\gamma_5 \psi_\lambda = \psi_{-\lambda}$, $\langle \psi_\lambda | \gamma_5 | \psi_\lambda \rangle = 0$ and $\langle \psi_\lambda | \gamma_5 | \psi_{-\lambda} \rangle = 1$. As a result, the zero modes are chiral and the number of the zero modes gives the topological charge. This is the index theorem. $\gamma_5(\cancel{D} + m)$ is the Hermitian Dirac operator with mass. It can be shown that the eigenvalues λ_H are related to the eigenvalues of the massless operator λ by $\lambda_H^2 = \lambda^2 + m^2$. The anti-commutator can be easily calculated to be $\{\gamma_5(\cancel{D} + m), \gamma_5\} = 2m$. The chirality can be obtained:

$$\langle \psi_{\pm\sqrt{\lambda^2+m^2}}^H | \gamma_5 | \psi_{\pm\sqrt{\lambda^2+m^2}}^H \rangle = \frac{m}{\lambda_H} = \frac{m}{\pm\sqrt{\lambda^2+m^2}} \quad (3.1)$$

Note that the mass introduces a scale on which the chirality depends. For all eigenvectors with $\lambda_H \approx m$, $\lambda \ll m$, the chirality is close to ± 1 . This is very different from the massless results.

In fact, the eigenvectors for the Dirac operator with the mass term can be obtained from the eigenvectors for the massless operator by a rotation:

$$\begin{aligned} \psi_{\sqrt{\lambda^2+m^2}}^H &= \frac{1}{\sqrt{2}}(e^{i\frac{\theta}{2}} \psi_\lambda + e^{-i\frac{\theta}{2}} \psi_{-\lambda}) \\ \psi_{-\sqrt{\lambda^2+m^2}}^H &= \frac{1}{\sqrt{2}}(e^{i\frac{\theta}{2}} \psi_\lambda - e^{-i\frac{\theta}{2}} \psi_{-\lambda}) \end{aligned} \quad (3.2)$$

where θ is given by $e^{i\theta} = \frac{m+i\lambda}{\sqrt{m^2+\lambda^2}}$. In general, for two operators with mass m_1 and m_2 , we have:

$$\begin{aligned} \langle \psi_{\sqrt{\lambda^2+m_1^2}}^H | \psi_{\sqrt{\lambda^2+m_2^2}}^H \rangle &= \cos(\theta_2 - \theta_1) \\ \langle \psi_{\sqrt{\lambda^2+m_1^2}}^H | \psi_{-\sqrt{\lambda^2+m_2^2}}^H \rangle &= i \sin(\theta_2 - \theta_1) \end{aligned} \quad (3.3)$$

For domain wall lattices, the Hermitian operator is $D_{DWF}^H = \gamma_5 R_5 D_{DWF}(m)$. The eigenvalue Λ should have the following form [4] for the low lying eigenvectors:

$$\Lambda^2 = n^2(\lambda^2 + (\delta m + m)^2) \quad (3.4)$$

Here, m is the input mass. n , δm and λ are the scale factor, the residual mass and the eigenvalue in the massless continuum, which have to be fitted. The fit of the eigenvalues are shown in Fig 1. The points are the calculated eigenvalues on the lattice for the different input masses. For each input mass, the 10 lowest eigenvalues are plotted (some of the eigenvalues are very close). We fit equation (3.4) for the eigenvalues of the different input masses. The curves are then plotted according to equation (3.4). It can be seen that the equation (3.4) describes the eigenvalues very well. The fitted residual masses are plotted against L_5 in the right graph of Fig 1. The residual mass

decreases inversely with L_5 which agrees with the understanding of the domain wall lattices. The graphs are for the configurations listed in the caption but the results are similar for all the ensembles and configurations.

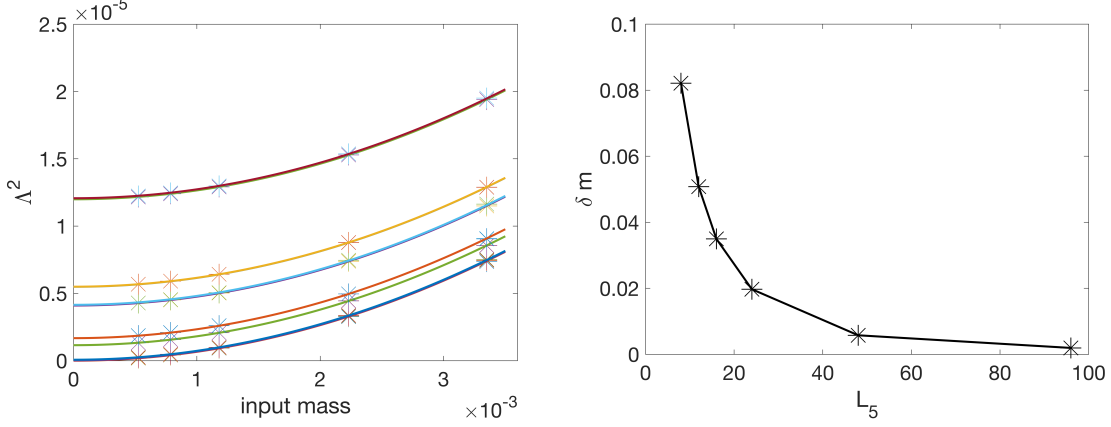


Figure 1: Left: eigenvalues of the lattice operator for different input masses, 24ID $a^{-1} \approx 2\text{GeV}$ ensemble, configuration 800; right: fitted residual mass as a function of L_5 , 12ID ensemble, configuration 700

The anti-commutation relation for the lattice Hermitian Dirac operator is: $\{D_{DWF}, \Gamma_5\} = 2m_f Q^{(w)} + 2Q^{(mp)} \equiv 2Q$, where $Q^{(w)}$ and $Q^{(mp)}$ are defined in [4]. Γ_5 is 1 for $s \geq L_5/2$ and -1 for $s < L_5/2$. This means that the chirality of the eigenvector follows:

$$\langle \Psi_i | \Gamma_5 | \Psi_i \rangle = \frac{\langle \Psi_i | Q | \Psi_i \rangle}{\Lambda_i} \quad (3.5)$$

When the numerator on the right hand side is constant for different eigenvectors, the chirality of the eigenvectors will be anti-proportional to the eigenvalues. This is the analog of equation (3.1) for the Dirac operator with mass in the continuum. In Fig 2, we show $1/\langle \Psi_i | \Gamma_5 | \Psi_i \rangle$ against the eigenvalues. The linear relationship shows that $\langle \Psi_i | Q | \Psi_i \rangle$ is indeed constant for different eigenvectors. Under this condition, when the mass increases, there are more eigenvectors with chirality close to 1 because there are more eigenvalues that are close to the mass. This explains that why there are multiple negative and positive chiral modes for the heavy mass. The results are similar for the other ensembles and configurations.

We are also able to study how the eigenvectors themselves change when the mass is changed and we compare the results to equation (3.2) and (3.3) in the continuum limit. In Fig 3, we show the inner product between eigenvectors for different masses. The x and y axis are the index of the eigenvectors of the different input masses. A good agreement with equation (3.2) and (3.3) is found for 24ID $a^{-1} \approx 2\text{GeV}$. For the 12ID $a^{-1} \approx 1\text{GeV}$, the agreement is poor which means that for the coarse lattice, it's further away from the continuum limit.

For finite L_5 , the residual mass makes it hard to get the true zero-modes. To understand the L_5 effect, we calculate the eigenvectors at different L_5 . In Fig 4, we show the matrix element $\langle \Psi_i | \Gamma_5 | \Psi_j \rangle$ where the diagonal elements are the chirality. For small L_5 , it can be seen that there are both positive and negative modes because of the large residual mass. When L_5 is increased, these modes gradually disappear. When $L_5 = 192$, there is one distinct zero modes. However, large mixing can still be seen which means that it's very hard to get rid of the residual mass effect.

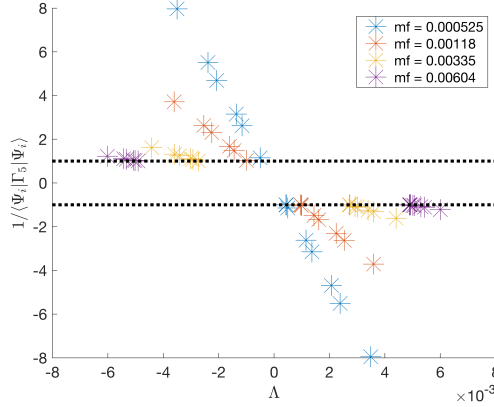


Figure 2: $1/\langle\Psi_i|\Gamma_5|\Psi_i\rangle$ as a function of eigenvalues, 24ID $a^{-1} \approx 2\text{GeV}$ ensemble, configuration 800

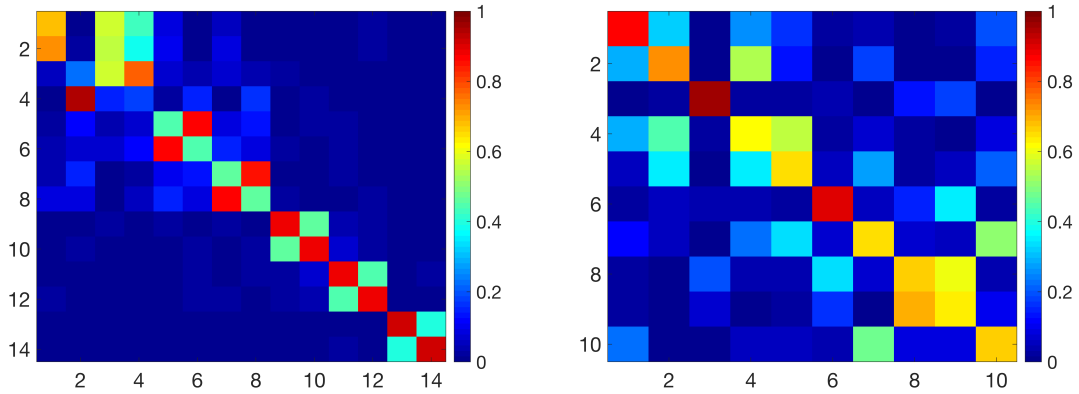


Figure 3: Left: Inner product between the eigenvectors with $m = 0.000525$ and $m = 0.00604$ for the 24ID, $a^{-1} \approx 2\text{GeV}$ ensemble, config 800; right: Inner product between eigenvectors with $m = 0.01$ and $m = 0.02$ for the 12ID ensemble, config 700

Lastly, we calculate the net topological charge by counting the net chiral modes. We consider chiral modes ($|\langle\Psi_i|\Gamma_5|\Psi_i\rangle| \geq 0.9$) and round the chirality to ± 1 . For the results from the field strength ($F\tilde{F}$), we first ran the Wilson flow with the flow time $t = 5.3$. The results are in the left graph of Fig 5 and one can see that the results are similar. However, for the eigenvectors, the measurements are done on the original lattices without smearing.

In summary, the eigenvalues and the chirality of the domain wall operator are described by the massive Dirac operator in the continuum. The finite L_5 brings in a mass scale and the massless limit is hard to reach. However, we obtained the detailed topological properties without the smearing.

4. From eigenvectors to the quark bilinear

In order to connect the topological properties and η' , we need to compare our results with the correlators to which the masses are fitted. Here we consider the quark bilinear $\sum_{\vec{x}, \vec{y}} \langle \bar{q}(\vec{x}, t) \gamma_5 q(\vec{y}, t) \rangle$ on the time slice which contributes significantly to the calculation of m_η and m'_η . The direct

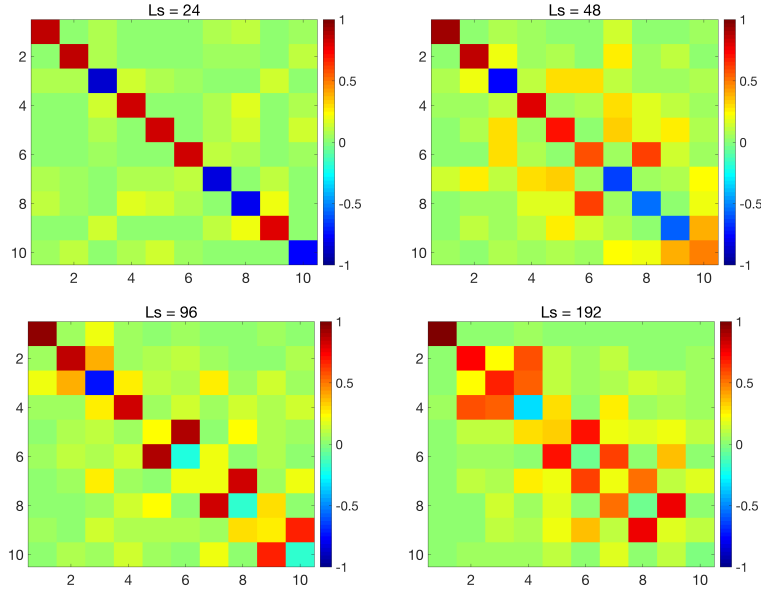


Figure 4: $\langle \Psi_i | \Gamma_5 | \Psi_j \rangle$ for different L_5 , 12ID ensemble, configuration 700

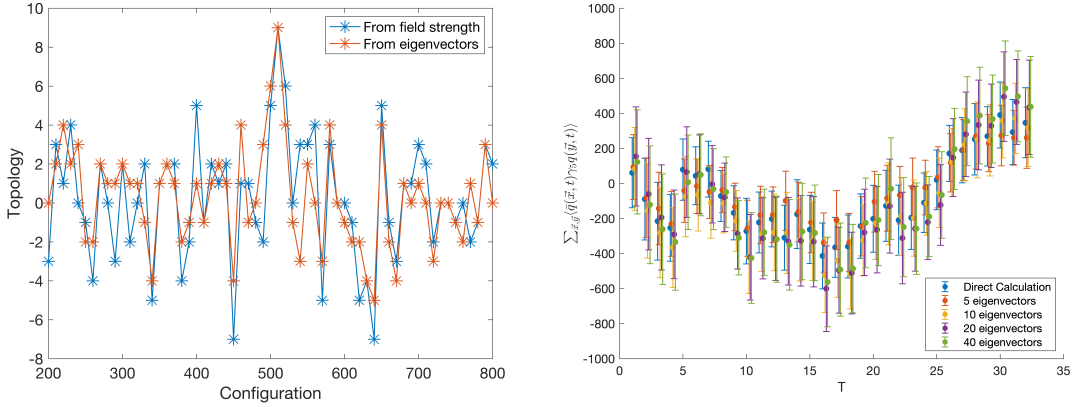


Figure 5: Left: topological charge calculated from the eigenvectors and the field strength; right: the quark bilinear calculated from the eigenvectors and the direct calculation. Both results are for 12ID ensemble, configuration 200 to 800 with a separation of 10

calculation is obtained by applying the inverse of \mathcal{D} to a wall source. However, one can also obtain the results by using the near-zero eigenvectors. The idea is very similar to the low-mode approximation. The formula is:

$$\sum_{\vec{x}, \vec{y}} \langle \bar{q}(\vec{x}, t) \gamma_5 q(\vec{y}, t) \rangle = \sum_n \frac{\text{Tr}(\sum_{\vec{x}, \vec{y}} (\Psi_n^\dagger(\vec{x}, t) \Psi_n(\vec{y}, t)))}{\Lambda_n} \quad (4.1)$$

We use different number of eigenvectors and the results are shown in Fig 5. Note that the results from the eigenvectors could approximate the direct calculation very well. It's interesting that we can approximate the direct calculation with only 5 eigenvectors. This shows that it's really topo-

size	a^{-1}	m_π	m_η	$m_{\eta'}$	θ
24x64	1	0.140	0.523(25)	0.924(113)	-18.6(6.7) $^\circ$
12x32	1	0.300	0.551(29)	1.17(24)	-11.3(5.0) $^\circ$
Experiment	-	-	0.548	0.958	-10 $^\circ \sim$ -20 $^\circ$

Table 2: $m_\eta, m_{\eta'}$ and the mixing angle θ

logical zero modes that are involved in this quark bilinear and thus $m_{\eta'}$.

5. η and η' mass

The calculation for $m_\eta, m_{\eta'}$ and the mixing angle θ is the same as [5] which we followed [2]. In table 2, we show the results for the 12ID ensemble and 24ID coarse ensemble. The results for the 24ID ensemble are the same as [5] and we include the results for the 12ID ensemble here. Although the results agree with the theoretical values, the error for η' is particularly large. We showed that there might be long autocorrelation in [5]. To investigate the autocorrelation in details, we believe the low lying eigenvectors studied in this proceeding will be a very effective tool.

6. Conclusion and outlook

We investigated the properties of the zero-mode eigenvectors of the Hermitian domain wall Dirac operator. We find that eigenvalues and chirality properties are very similar to those of the Hermitian massive Dirac operator in the continuum. For the lattice operator, because of the finite L_5 effect, there is always a mass scale in the eigenvectors. However, we can still obtain topological properties from the low-lying eigenvectors. The advantage of using the operator is that no smearing is required and the detailed properties can be obtained.

We also obtain the quark bilinear $\sum_{\vec{x}, \vec{y}} \langle \bar{q}(\vec{x}, t) \gamma_5 q(\vec{y}, t) \rangle$ using the eigenvectors. This is a direct evidence showing that topological properties affect the Fermion propagator and η' . We are also able to obtain m_η and $m_{\eta'}$. However, the current results for the masses are not very satisfying because of topological issues. We believe that once we have more statistics and use the tools of eigenvectors to study the topological evolution in more details, we will be able to obtain more precise results for η' and η . Furthermore, we are also trying to use different operators to further constrain the masses. These investigations are in the process and they'll give us a better understanding of the topological properties of the fields and η' and η .

References

- [1] G. 't Hooft, *Symmetry Breaking through Bell-Jackiw Anomalies*, *Phys. Rev. Lett.* **37**, 8 (1976).
- [2] N. Christ, et. al., *The η and η' Mesons from Lattice QCD*, *Phys. Rev. Lett.* **105**, 241601 (2010).
- [3] P. A. Boyle, et al., *Low Energy Constants of SU(2) Partially Quenched Chiral Perturbation Theory from $N_f = 2 + 1$ Domain Wall QCD*, *Phys. Rev.* **D93**, 054502 (2016).
- [4] G. Liu, *Quark eigenmodes and lattice QCD*, UMI-31-04827.
- [5] D. Guo, *The η' mass on 2+1 flavor DWF lattices*, *PoS LATTICE 2018*, 046 (2018).